Automatic Computation of Ejection Fraction using Spatio-Temporal Information

A. S. Pednekar[1,2], R. Muthupillai[2,3], B. Cheong[2], S. D. Flamm[2,4]

[1]Philips Medical Systems, Bothell, WA, United States, [2]Department of Radiology, St.Luke's Episcopal Hospital and Texas Heart Institute, Houston, TX, United States, [3]Philips Medical Systems, Cleveland, OH, United States, [4]Department of Cardiology, St.Luke's Episcopal Hospital and Texas Heart Institute, Houston, TX, United States

Abstract: The current clinical practice of manually tracing the endocardium and blood pool to compute the left ventricular (LV) ejection fraction (EF) from cine-magnetic resonance images (cine-MRI) is labor intensive, time consuming, and operator dependent. We used spatio-temporal information in the LV cine-MRI to automatically estimate the EF in 64 subjects (21 normal volunteers, and 43 patients). This entirely data-driven, multi-step approach incorporates *apriori* geometric information from the acquisition and spatial-temporal information that is intrinsic to cardiac cine-MR. The results show that the mean bias values determined by Bland-Altman (BA) analysis for volumetric computations using our algorithm for end-diastolic (ED) and end-systolic (ES) phases and hence for EF are in close agreement with inter- and intra-observer variability.

Introduction: A reliable automatic method to segment the LV cavity in short-axis cine-MR would eliminate the cumbersome practice of manual segmentation by experts and would reduce intra- and inter-observer variability. Recent efforts for automatic delineation of the LV endocardial contour, circumscribing the papillary muscles and trabeculae, involve energy minimization between the image-derived features and the statistical LV shape [1-5]. We propose a data driven, 2D slice-by-slice approach incorporating spatio-temporal information intrinsic to cardiac cine images. The purpose of this paper is to describe our segmentation approach and to investigate its clinical feasibility.

Materials and Methods: The studies were performed on 21(13m/8f) healthy volunteers, with a mean age of 34 years (range 22-54), and 43 years (10m/3f) clinical patients, with a mean age of 55 (range 17-78), all of whom were evaluated for LV dysfunction.

MR Sequences: All subjects were imaged on a 1.5T, Philips Gyroscan NT-Intera, using a 5-element phased-array surface coil. Vector-cardiographic (VCG) gated cine SSFP images (TR/TE/flip: 3.2 msec/1.6 msec/60 deg; temporal resolution: 40 msec; acquired spatial resolution: 1.25 x 1.25 x 8 mm^3) were acquired in the following order: a vertical long-axis (VLA) view, a 4-chamber (4CH) view, and a series of 10 to 13 contiguous short-axis (SA) slices covering the entire LV from apex to base (the level of the mitral valve annulus). Each cine slice was acquired during suspended respiration (10-12 heartbeats).

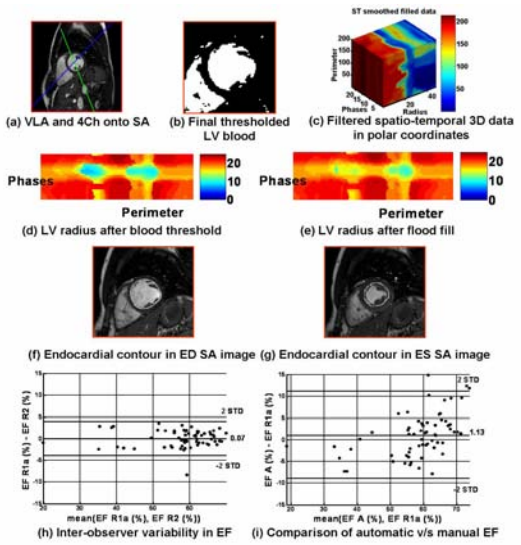

Figure 1: Algorithmic overview and Bland-Altman analyses.

Algorithm: The algorithm involved the following steps 1) Maping the intersection line of the VLA and 4CH scout images onto the stack of SA images to locate the LV (Fig. 1a); (2) threshold the LV blood using a histogram of the 3D spatio-temporal data; (3) identify the LV in each SA slice from base to apex using a cross-section of VLA and 4CH, thresholded blood, and progressive 3D geometric continuity constraints; (4) segment the LV using dynamic weights fuzzy connectedness algorithm; (5) successively threshold the LV region of interest (ROI) to compute LV blood and myocardial intensity statistics (Fig. 1b); (6) convert the data for the LV ROI into polar coordinates and compute the ED endocardial contour as the optimal path using dynamic programming; (7) perform 3D filtering on spatio-temporal data in the polar coordinates with the center of the ED LV as the origin (Fig. 1c) and threshold the LV blood based on the histogram (Fig. 1d); (8) perform a 3D hole filling on the thresholded LV blood (Fig. 1e); and (9) compute the endocardial contours for the ED and ES phases (Fig. 1f-g).

Results: A total of 1078 slices (343 slices from 21 volunteers and 735 slices from 43 patients) were analyzed using our algorithm (A) and manually by two experts (R1 and R2). The first expert repeated the contours after two weeks (R1a and R1b). Some representative images describing the segmentation process are shown in Fig. 1, and the BA comparisons are shown in Table 1.

		A/R1a		A/R2		R1a/R2		R1a/R1b	
		Bias	2SD	Bias	2SD	Bias	2SD	Bias	2SD
ED	Basal (ml)	-1.62	7.05	-1.26	7.37	0.37	7.99	-4.46	7.06
	Mid-cavity (ml)	-2.55	7.38	-4.67	7.65	-2.12	4.43	-1.79	4.78
	Apical (ml)	-1.31	6.79	-4.53	7.84	-3.21	6.21	-2.01	5
ES	Basal (ml)	-3.24	5.68	-1.84	6.9	1.4	5.2	-0.85	4.66
	Mid-cavity (ml)	0.02	13.03	-2.27	13.67	-2.28	5.4	-1.87	5.59
	Apical (ml)	-0.51	8.03	-1.99	7.46	-1.49	4.26	-1.51	4.5
	EDV (ml)	-5.49	13.52	-10.45	16.26	-4.96	10.49	-8.26	12.62
	ESV (ml)	-3.73	17.07	-6.1	17.16	-2.37	8.96	-4.22	11.63
	EF (%)	1.13	10.01	1.2	10.1	0.07	3.93	0.05	4.98

Table 1: Bland-Altman comparisons between the automatic and manual methods for 3 different sections of the LV correlated to the papillary muscles and trabeculae.

Discussion: The results show that the mean bias as determined by BA for volumetric computations using our algorithm for the ED and ES phases for all the 3 LV sections to be in close agreement with inter- and intra-observer variability (<1.2% EF; <8 ml/5% EDV; 5 ml/7% ESV). In the ED phase, independent of the anatomic location of the LV (i.e., basal, mid-cavity, or apical), the limits of agreement were small (<5% EDV). However, in the ES phase, the limits of agreement for the mid-cavity (<19% ESV) and apical (<11% ESV) slices were twice that of the inter- and intra-observer variability but were still less than 25% for the ESV.

Conclusion: Our clinical evaluation in 64 subjects using BA analysis show that the data-driven, slice-by-slice segmentation approach utilizing *apriori*, and spatio-temporal information can estimate the EDV, ESV, and EF in close agreement with inter- and intra-observer variability.

References:

1. H. van Assen, M. Danilouchkine, F. Behloul, H. Lamb, R. van der Geest, J. Reiber, and B. Lelieveldt, "Cardiac LV segmentation using a 3D active shape model driven by fuzzy inference," in Proc. Medical Image Computing and Computer-Assisted Intervention, 2003, pp. 533–540.
2. M. Kaus, J. von Berg, W. Niessen, and V. Pekar, "Automated segmentation of the left ventricle in cardiac MRI," Medical Image Analysis, vol. 8, pp. 245–254, 2004.
3. M. Lorenzo-valdes, G. Sanchez-Ortiz, A. Elkington, R. Mohiaddin, and D. Rueckert, "Segmentation of 4d cardiac MR images using a probabilistic atlas," Medical Image Analysis, vol. 8, pp. 255–265, 2004.
4. J. Lotjonen, S. Kivisto, J. Koikkalainen, D. Smutek, and K. Laurema, "Statistical shape model of atria, ventricles and epicardium from short- and long-axis MR images," Medical Image Analysis, vol. 8, pp. 371–86, 2004.
5. M. Stegmann and D. Pedersen, "Bi-temporal 3D active appearance models with applications to unsupervised ejection fraction estimation" in Proc. of SPIE vol. 5747, Feb 2005.
6. A. Pednekar and I. Kakadiaris, Image segmentation based on fuzzy connectedness using dynamic weights, IEEE Trans on Image Processing, In print.